J. Am. Chem. Soc. **1991**, *113*, 1627-1635

Influence of Hydrogen Bonding on the Formation of Boat and Chair Conformations of Six-Membered Rings in Spirocyclic Tetraoxyphosphoranes[1]

Roberta O. Day, K. C. Kumara Swamy,[2] Lisa Fairchild, Joan M. Holmes, and Robert R. Holmes*

Contribution from the Department of Chemistry, University of Massachusetts, Amherst, Massachusetts 01003.

Received July 16, 1990

Abstract: Oxidative addition reactions of the monocyclic phosphite, ($Me_2C_3H_4O_2P$(O-Xyl), with aminophenol and aminocresol derivatives yielded the new bicyclic tetraoxyphosphoranes containing saturated six-membered rings, ($C_5H_{10}O_2$)(Xyl-O)P(1-O-2-NHC_6H_4) (**1**) and ($C_5H_{10}O_2$)(Xyl-O)P(1-O-2-NH-X-MeC_6H_3) (X = 4 (**2**), 5 (**3**)). Hydrogen bonding was introduced via N–H---O intermolecular interactions to ascertain their importance as a structural determinant. X-ray analysis revealed phosphoranes in a trigonal-bipyramidal framework with the rings positioned in axial-equatorial sites. Hydrogen bonding between molecular units gave rise to helical chain form **1** and dimeric forms **2** and **3**. The phosphorinane rings were present in a twist-chair conformation for **1** and in both twist-chair and twist-boat conformations for **2** and **3**. Variable-temperature solution-state ^1H and ^{13}C NMR supported retention of the solid-state structures and the presence of hydrogen bonding. Activation energies for intramolecular ligand exchange suggested at least a 10-kcal/mol requirement for reorientation of the six-membered ring in these phosphoranes to diequatorial locations in a TBP. The relevance of these results to pentaoxyphosphorane intermediates in c-AMP enzyme reactions is discussed. **1** crystallizes in the tetragonal space group $P4_1$ with $a = b = 10.772$ (3) Å, $c = 16.917$ (3) Å, and $Z = 4$. **2** crystallizes in the triclinic space group $P\bar{1}$ with $a = 12.529$ (2) Å, $b = 14.638$ (4) Å, $c = 14.842$ (3) Å, $\alpha = 60.78$ (2)°, $\beta = 76.21$ (2)°, $\gamma = 59.25$ (2)°, and $Z = 4$. **3** crystallizes in the monoclinic space group $P2_1/c$ with $a = 21.607$ (5) Å, $b = 14.901$ (4) Å, $c = 13.679$ (3) Å, $\beta = 108.30$ (2)°, and $Z = 8$. The final conventional unweighted residuals are 0.035 (**1**), 0.041 (**2**), and 0.049 (**3**).

Introduction

Previous work[1b,3–7] on cyclic pentaoxyphosphoranes which have ring systems varying from five- to eight-membered has revealed the principal structural features attributable to these compounds. Those phosphoranes which contain six-membered rings comprise a class of compounds that serve as models for intermediates or transition states in reactions of the nucleoside cyclic 3′,5′-monophosphate, c-AMP.[8–10] We have examined the molecular structures of eight[1b,3–6] such members by X-ray crystallography and find that the rings of both monocyclic[5] and spirocyclic[1b,4] derivatives are positioned at apical-equatorial sites of a trigonal bipyramid. In the case of derivatives with six-membered saturated rings,[1b,3–7] the rings reside in boat or twist boat conformations with the axial oxygen atoms and carbon atoms opposite them at the prow and the stern of the boat, e.g., A[5] and B.[4]

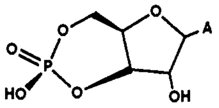

c-AMP

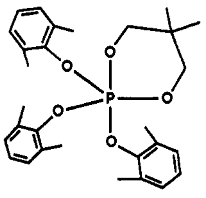

A[5]

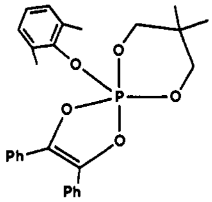

B[4]

Additional X-ray analyses on members C–F[1b,11,12] which have sulfur or nitrogen atoms in place of oxygen show that these structural preferences are maintained. Introduction of a trans-fused five-membered ring as is present in c-AMP also does not cause any significant structural variation. The first X-ray structures of three such members have recently been reported, G,[1b,13] H,[14a] and one that closely resembles H.[14b]

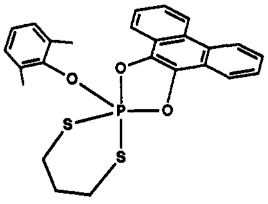

C[11]

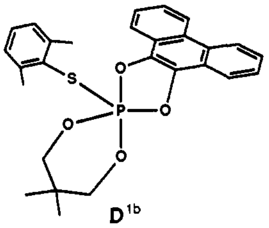

D[1b]

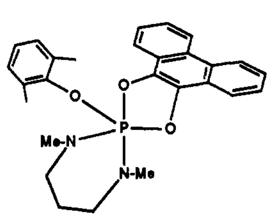

E[1b]

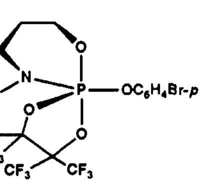

F[12]

---

(1) (a) Pentacoordinated Molecules 85. (b) Part 84: Holmes, R. R.; Kumara Swamy, K. C.; Holmes, J. M.; Day, R. O. *Inorg. Chem.*, in press. (c) Holmes, R. R.; Day, R. O.; Fairchild, L.; Kumara Swamy, K. C.; Holmes, J. M.; Burton, S. D. Presented in part at the 199th National Meeting of the American Chemical Society, Boston, MA, April 1990; INOR 503.

(2) Present address: School of Chemistry, University of Hyderabad, Hyderabad 500 134, India.

(3) (a) Kumara Swamy, K. C.; Burton, S. D.; Holmes, J. M.; Day, R. O.; Holmes, R. R., presented in part at the XI International Conference on Phosphorus Chemistry, Tallinn, Estonia (SSR/USSR), July 1989: Abstract 2-22. (b) Kumara Swamy, K. C.; Burton, S. D.; Holmes, J. M.; Day, R. O.; Holmes, R. R. *Phosphorus Sulfur Silicon* **1990**, *49/50*, 367.

(4) Kumara Swamy, K. C.; Day, R. O.; Holmes, J. M.; Holmes, R. R. *J. Am. Chem. Soc.* **1990**, *112*, 6095.

(5) Burton, S. D.; Kumara Swamy, K. C.; Holmes, J. M.; Day, R. O.; Holmes, R. R. *J. Am. Chem. Soc.* **1990**, *112*, 6104.

(6) Kumara Swamy, K. C.; Burton, S. D.; Holmes, J. M.; Day, R. O.; Holmes, R. R. *Phosphorus Sulfur Silicon* **1990**, *53*, 437.

(7) Schomburg, D.; Hacklin, H.; Röschenthaler, G.-V. *Phosphorus Sulfur* **1988**, *35*, 241.

(8) van Ool, P. J. J. M.; Buck, H. M. *Recl. Trav. Chim. Pays-Bas* **1981**, *100*, 79.

(9) van Ool, P. J. J. M.; Buck, H. M. *Eur. J. Biochem.* **1982**, *121*, 329.

(10) Mehdi, S.; Coderre, J. A.; Gerlt, J. A. *Tetrahedron* **1983**, *39*, 3483 and references cited therein.

(11) Kumara Swamy, K. C.; Holmes, J. M.; Day, R. O.; Holmes, R. R. *J. Am. Chem. Soc.* **1990**, *112*, 6092.

(12) Barlow, J. H.; Bone, S. A.; Russell, D. R.; Trippett, S.; Whittle, P. J. *J. Chem. Soc., Chem. Commun.* **1976**, 1031.

(13) First reported at the 200th National Meeting of the American Chemical Society, Washington, DC, August 1990; INOR 26.

0002-7863/91/1513-1627$02.50/0

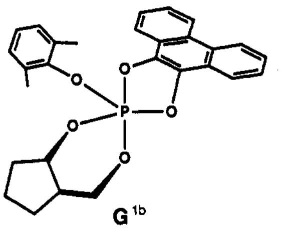

G[1b]

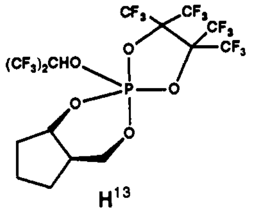

H[13]

Variable-temperature NMR data[1b-6] indicate that the solid-state structures are retained in solution and further reveal intramolecular ligand exchange processes (Berry pseudorotation[15]) that allow an estimation of the energy required[4,5] to promote a ground-state axial-equatorial six-membered ring in a boat conformation to locate in diequatorial sites of a trigonal bipyramid, presumably in a chair conformation. In a comparative ^{19}F NMR study of five- and six-membered-ring systems in pentaoxyphosphoranes, Trippett[16] obtained an exchange barrier for the process ax-eq ⇌ eq-eq of 17.4 kcal/mol for I compared to only 6.1 kcal/mol for J.

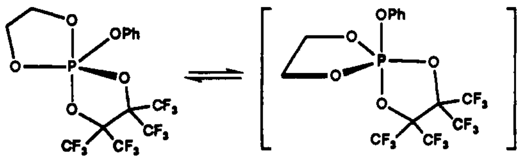

I

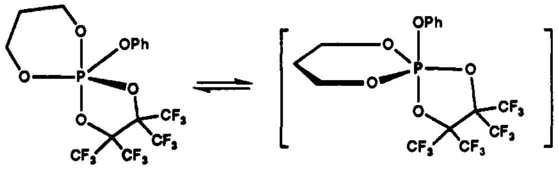

J

Bentrude and co-workers[17,18] carried out the most detailed solution NMR studies and established retention of twist conformations of six-membered rings in TBP environments. However, in spite of the diversity of cyclic phosphorane systems now studied, apical-equatorial ring placement is uniformly found by X-ray analysis. In an isolated NMR investigation, Denney et al.[19] report variable-temperature data consistent with diequatorial location of seven- and eight-membered rings in a TBP for monocyclic pentaoxyphosphoranes containing perfluoroalkoxy ligands, OCH_2CF_3.[20]

In a continuing effort of examining conditions influencing the structure of cyclic oxyphosphoranes, we report our initial results on the role of hydrogen bonding as a factor inducing conformational change. An understanding of the latter influence is of considerable significance in modeling enzymatic activity of c-AMP.[10,21] In the present study, hydrogen bonding is introduced via the N–H group of *o*-aminophenols that are used as reactants with 2-(2,6-dimethylphenoxy)-5,5-dimethyl-1,3,2-dioxaphosphorinane. The new spirocyclic tetraoxyphosphoranes formed, **1–3**, are subjected to X-ray and NMR analyses.

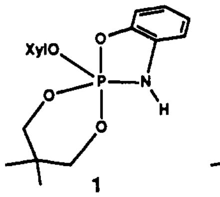

1

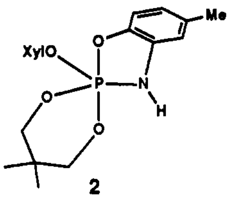

2

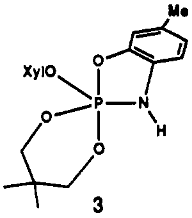

3

Experimental Section

Chemicals were obtained from Aldrich, Fisher Scientific, or Fluka and used without further purification. Solvents were of HPLC grade (Fisher Scientific). Further purification was done according to standard procedures.[22a,b] 2-(2,6-Dimethylphenoxy)-5,5-dimethyl-1,3,2-dioxaphosphorinane, $(Me_2C_3H_4O_2)P(O\text{-}Xyl)$ (**4**), was synthesized from the reaction of the chloro derivative with 2,6-dimethylphenol according to our previous procedure.[4]

^{1}H and ^{13}C NMR spectra were recorded on a Varian Associates XL 300 FT-NMR or a Varian Associates XL 200 FT-NMR and referenced relative to Me_4Si. ^{31}P NMR spectra were recorded on the Varian Associates XL 300 FT-NMR spectrometer. Chemical shifts for ^{31}P NMR spectra were obtained by setting triphenyl phosphate ($CDCl_3$) at −18.0 ppm[22c] and are referenced to 85% H_3PO_4 with negative shifts upfield. Temperature calibration was accomplished by using an ethylene glycol sample with a calibration error at ±0.5 °C.

Preparation of $(C_5H_{10}O_2)(Xyl\text{-}O)P(1\text{-}O\text{-}2\text{-}NHC_6H_4)$ (1). To a solution of 2-(2,6-dimethylphenoxy)-5,5-dimethyl-1,3,2-dioxaphosphorinane (**4**) (1.70 g, 6.69 mmol) and *o*-aminophenol (0.73 g, 6.69 mmol) in dimethyl ether (80 mL) maintained at −55 °C a solution of *N*-chlorodiisopropylamine (0.92 g, 6.80 mmol) in diethyl ether (20 mL) was added dropwise over a period of 10 min under a nitrogen atmosphere. The mixture was brought to 20 °C and maintained at this temperature for 12 h. It was then filtered under a blanket of nitrogen and the solvent completely removed from the filtrate. The residue was redissolved in diethyl ether (100 mL) and filtered. The filtrate, upon slow evaporation of the solvent, afforded a crystalline product of **1**, mp 184–187 °C (1.30 g, 54%). ^{1}H NMR ($C_6D_5CD_3$, ppm, 15 °C): 0.62 (s, 3 H, $CH_2C(CH_3)_2$), 0.97 (s, 3 H, $CH_2C(CH_3)_2$), 2.27 (d, J = 1.2 Hz, 6 H, $C_6H_3(CH_3)_2$), 3.57 (dd, $^3J(P\text{-}H_X)$ = 23.1 Hz, $^2J(H_A\text{-}H_X)$ = 10.8 Hz, 2 H, $OCH_2(X)$), 4.07 (t or dd, $^3J(P\text{-}H_A) = {}^3J(H_A\text{-}H_X)$ = 10.2 Hz, 2 H, $OCH_2(A)$), 5.29 (d, $^2J(P\text{-}H)$ = 19.9 Hz, 1 H, NH), 6.30–7.20 (m, 7 H, H(Ar)). ^{31}P NMR ($CDCl_3$) −57.9 ppm. ^{13}C NMR ($C_6D_5CD_3$, 25 °C) 16.95 ($OC_6H_3C(CH_3)_2$), 22.10, 23.44 ($C(CH_3)_2$), 31.52 ($C(CH)_2$), 76.16 ppm (OCH_2). Aromatic carbons were masked by the peaks due to toluene-d_8. Anal. Calcd for $C_{19}H_{24}O_4NP$: C, 63.16; H, 6.65; N, 3.88. Found: C, 63.24; H, 6.66; N, 3.90.

Preparation of $(C_5H_{10}O_2)(Xyl\text{-}O)P(1\text{-}O\text{-}2\text{-}NH\text{-}4\text{-}MeC_6H_3)$ (2). The preparation of **2** from **4** and 2-amino-*p*-cresol was conducted similar to that for **1** except a more extensive workup was required. A description follows. A noncrystalline white precipitate was removed from the solute using Schlenk filtration techniques for three successive filtrations. Before each filtration, precipitate was allowed to form in the filtrate due to evaporation over several days under a positive nitrogen flow. The filtrate from the third filtration afforded crystals of **2**. The crystals were covered with an oily substance which could not be washed off with ether without dissolving the crystals as well. These crystals melted over the range 100–125 °C (0.44 g, 12%). ^{1}H NMR ($C_6H_5CD_3$, 23 °C) 0.64 (s, 3 H, $CH_2C(CH_3)_2$), 0.98 (s, 3 H, $CH_2C(CH_3)_2$), 2.08 (s, 3 H, $CHCCH_3$), 2.28 (d, 6 H, J = 1.5 Hz, $C_6H_3(CH_3)_2$), 3.62 (dd, $^3J(P\text{-}H_B)$ = 22.9 Hz, $^2J(H_A\text{-}H_B)$ = 10.4 Hz, 2 H, $OCH_2(B)$), 4.08 (t or dd, $^3J(P\text{-}H_A) = {}^3(H_A\text{-}H_B)$ = 10.4 Hz, 2 H, 2 H, $OCH_2(A)$), 5.30 (d, $^2J(P\text{-}H)$ = 19.9 Hz, 1 H, NH), 6.16–7.10 ppm (m, 6 H, H(Ar)). ^{31}P NMR ($CDCl_3$) −57.7 ppm. Anal. Calcd for $C_{20}H_{26}O_4PN$: C, 64.00; H, 6.98. Found: C, 63.87; H, 7.15.

Preparation of $(C_5H_{10}O_2)(Xyl\text{-}O)P(1\text{-}O\text{-}2\text{-}NH\text{-}5\text{-}MeC_6H_3)$ (3). The preparation of **3** from **4** and 6-amino-*m*-cresol was carried out similar to that for **2** in the reaction scheme as well as in the product workup. The resulting crystals melted over the range 130–150 °C (0.48 g, 14%). ^{1}H

---

(14) (a) Yu, J. H.; Sopchik, A. E.; Arif, A. M.; Bentrude, W. G. *J. Org. Chem.* **1990**, *55*, 3444. (b) Yu, J. H.; Arif, A. M.; Bentrude, W. G. *J. Am. Chem. Soc.* **1990**, *112*, 7451.

(15) Berry, R. S. *J. Chem. Phys.* **1960**, *32*, 933.

(16) Trippett, S. *Pure Appl. Chem.* **1974**, *40*, 595.

(17) Yu, J.-H.; Bentrude, W. G. *Tetrahedron Lett.* **1989**, *30*, 2195.

(18) Yu, J.-H.; Bentrude, W. G. *J. Am. Chem. Soc.* **1988**, *110*, 7897.

(19) Abdou, W. M.; Denney, D. B.; Denney, D. Z.; Pastor, S. D. *Phosphorus Sulfur* **1985**, *22*, 99.

(20) In a further report, van Ool and Buck (van Ool, P. J. J. M.; Buck, H. M. *Recl. Trav. Chim. Pays-Bas* **1984**, *103*, 119) stated that the trans-annelated phosphorane,

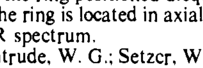

likely exists in a TBP with the ring positioned diequatorially. However, Yu et al. (ref 14) have shown the ring is located in axial-equatorial sites from the low-temperature ^{13}C NMR spectrum.

(21) Nelson, K. A.; Bentrude, W. G.; Setzer, W. N.; Hutchinson, J. P. *J. Am. Chem. Soc.* **1987**, *109*, 4058 and references cited therein.

(22) (a) Riddick, J. A.; Bunger, W. B., Eds. Organic Solvents. In *Physical Methods in Organic Chemistry*; Weissberger, Wiley Interscience: New York, 1970; Vol. II. (b) Vogel, A. I. *Textbook of Practical Organic Chemistry*; Lingman: London, 1978. (c) Emsley, J.; Hall, D. *The Chemistry of Phosphorus*; Wiley: New York, 1976; p 82.

Table I. Selected Distances (Å) and Angles (deg) for **1**[a]

atom 1	atom 2	distance	atom 1	atom 2	distance	atom 1	atom 2	distance	atom 1	atom 2	distance
P	O1	1.648 (3)	O1	C1	1.397 (8)	N	C11	1.393 (6)	C11	C12	1.385 (7)
P	O2	1.586 (3)	O2	C2	1.453 (7)	C1	C3	1.511 (9)	C11	C16	1.389 (7)
P	O3	1.615 (3)	O3	C31	1.407 (6)	C2	C3	1.495 (9)	C12	C13	1.373 (7)
P	O5	1.740 (3)	O5	C12	1.355 (5)	C3	C4	1.529 (9)	N	H1	0.85 (6)
P	N	1.654 (4)	H1	O2′	2.39 (6)	C3	C5	1.483 (9)	H1	O5′	2.35 (6)

atom 1	atom 2	atom 3	angle	atom 1	atom 2	atom 3	angle	atom 1	atom 2	atom 3	angle
O1	P	O2	98.3 (2)	P	O3	C31	127.9 (3)	C2	C3	C5	111.8 (5)
O1	P	O3	90.2 (2)	P	O5	C12	114.3 (3)	C4	C3	C5	109.5 (6)
O1	P	O5	175.1 (2)	P	N	C11	116.9 (3)	N	C11	C12	109.4 (4)
O1	P	N	87.6 (2)	P	N	H1	120. (4)	N	C11	C16	130.2 (5)
O2	P	O3	113.5 (2)	C11	N	H1	122. (4)	C12	C11	C16	120.3 (4)
O2	P	O5	85.1 (2)	O1	C1	C3	112.2 (5)	O5	C12	C11	111.7 (4)
O2	P	N	122.6 (2)	O2	C2	C3	114.4 (5)	O5	C12	C13	126.2 (4)
O3	P	O5	91.6 (2)	C1	C3	C2	103.1 (5)	C11	C12	C13	122.1 (4)
O3	P	N	123.6 (2)	C1	C3	C4	108.6 (5)	N	H1	O2′	162. (5)
O5	P	N	87.6 (2)	C1	C3	C5	115.5 (6)	N	H1	O5′	140. (5)
P	O1	C1	123.5 (4)	C2	C3	C4	108.0 (5)	P	O2	H1″	111. (1)
P	O2	C2	128.6 (3)					P	O5	H1″	107. (1)

[a] Estimated standard deviations in parentheses. The atom-labeling scheme is shown in Figure 1.

NMR ($C_6D_5CD_3$, 23 °C) 0.64 (s, 3 H, $CH_2C(CH_3)_2$), 0.97 (s, 3 H, $CH_2C(CH_3)_2$), 1.92 (s, 3 H, $CHCCH_3$), 2.29 (d, $J = 1.4$ Hz, 6 H, $C_6H_3(CH_3)_2$), 3.57 (dd, $^3J(P\text{-}H_B) = 22.9$ Hz, $^2J(H_A\text{-}H_B) = 10.8$ Hz, 2 H, OCH_2(B)), 4.08 (t, $J = 10.4$ Hz, 2 H, OCH_2(A)), 5.26 (d, $^2J(P\text{-}H) = 17.2$ Hz, 1 H, N*H*), 6.21–7.10 ppm (m, 6 H, H(Ar)). ^{31}P NMR ($CDCl_3$) −57.6 ppm. Anal. Calcd for $C_{20}H_{26}O_4PN$: C, 64.00; H, 6.98. Found: C, 63.77; H, 7.09.

X-ray Studies. All X-ray crystallographic studies were done with an Enraf-Nonius CAD4 diffractometer and graphite monochromated molybdenum radiation ($\lambda K\bar{\alpha} = 0.71073$ Å) at an ambient temperature of 23 ± 2 °C. Details of the experimental procedures have been described previously.[23]

Crystals were mounted in thin-walled glass capillaries which were sealed as a precaution against moisture sensitivity. Data were collected with use of the θ–2θ scan mode with $2\theta_{min} = 3°$ and $2\theta_{max} = 50°$, 43°, and 42° for **1** through **3**, respectively. No corrections were made for absorption. The structures were solved by use of direct methods and difference Fourier techniques and were refined by full-matrix least-squares methods.[24] All computations were performed on a Microvax II computer with the Enraf-Nonius SDP system of programs.

Crystals of all three compounds are colorless, but they appear tan in bulk due to the presence of an orange-brown oil on their surfaces.

X-ray Study for ($C_5H_{10}O_2$)(Xyl-O)P(1-O-2-NHC_6H_4) (1). The elongated polyfaceted crystal used for the X-ray study has approximate dimensions of 0.30 × 0.33 × 0.63 mm.

Crystal data for $C_{19}H_{24}O_4NP$ (1): tetragonal space group $P4_1$ [C_4^2—No. 76],[25] $a = b = 10.772$ (3) Å, $c = 16.917$ (3) Å, $Z = 4$, and $\mu_{MoK\bar{\alpha}} = 1.554$ cm^{-1}. A total of 1773 independent reflections ($+h$, $+k$, $+l$; $0kl$'s excluded) was measured.

The 25 independent non-hydrogen atoms were refined anisotropically. The 23 independent hydrogen atoms bonded to carbon were included in the refinement as fixed isotropic scatterers (ideal geometry or regularized difference Fourier geometry for xylyl methyl groups). The independent imino hydrogen atom was located on a difference Fourier synthesis and was refined as an isotropic scatterer was fixed B. The final agreement factors[26] were $R = 0.035$ and $R_w = 0.042$ for the 1058 reflections having $I \geq 3\sigma_I$. Refinement in the enantiomorphic space group, $P4_3$, led to the same values for R and R_w, with a slightly higher goodness of fit.

X-ray Study for ($C_5H_{10}O_2$)(Xyl-O)P(1-O-2-NH-4-MeC_6H_3) (2). The crystal used for the X-ray study was cut from a fused sticky polycrystalline mass and had dimensions of 0.18 × 0.38 × 0.50 mm.

Crystal Data for $C_{20}H_{26}O_4NP$ (2): triclinic space group $P\bar{1}$ [C_i^1—No. 2],[27] $a = 12.529$ (2) Å, $b = 14.638$ (4) Å, $c = 14.842$ (3) Å, $\alpha = 60.78$ (2)°, $\beta = 76.21$ (2)°, $\gamma = 59.25$ (2)°, $Z = 4$, and $\mu_{MoK\bar{\alpha}} = 1.518$ cm^{-1}. A total of 4655 independent reflections ($+h$, $\pm k$, $\pm l$) was measured. The 52 independent non-hydrogen atoms were refined anisotropically. The 52 independent hydrogen atoms were treated as described for **1**. The final agreement factors were $R = 0.041$ and $R_w = 0.053$ for the 3072 reflections having $I \geq 3\sigma_I$.

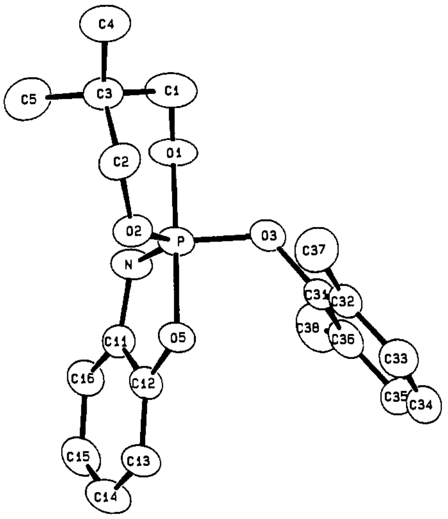

Figure 1. ORTEP plot of ($C_5H_{10}O_2$)(Xyl-O)P(1-O-2-NHC_6H_4) (**1**) with thermal ellipsoids at the 30% probability level. Hydrogen atoms are omitted for clarity.

X-ray Study for ($C_5H_{10}O_2$)(Xyl-O)P(1-O-2-NH-5-MeC_6H_3) (3). The irregularly shaped crystal used for the X-ray study was removed from a sticky mass of fused crystals with nonfaceted morphology and cut to approximate dimensions of 0.20 × 0.35 × 0.50 mm. Although the Niggli matrix suggested transformation to a C-centered orthorhombic cell, the diffraction symmetry and the systematic extinctions did not support this assignment.

Crystal Data for $C_{20}H_{26}O_4NP$ (3): monoclinic space group $P2_1/c$ [C_{2h}^5—No. 14],[28] $a = 21.607$ (5) Å, $b = 14.901$ (4) Å, $c = 13.679$ (3) Å, $\beta = 108.30$ (2)°, $Z = 8$, and $\mu_{MoK\alpha} = 1.482$ cm^{-1}. A total of 4447 independent reflections ($+h$, $+k$, $\pm l$) was measured.

During solution of the structure it became apparent that there was disorder in the phosphorinane ring containing P1. It was possible to resolve two positions for atom C12 of this ring, but only one set of positions was found for the remaining atoms. The thermal ellipsoids for the ring methyl substituent carbon atoms C14 and C15 suggest two unresolved sets of positions for these atoms. The disordered C12 was refined isotropically as two atoms (C12A and C12B) in half occupancy. The remaining 51 independent non-hydrogen atoms were refined anisotropically. The eight independent hydrogen atoms bonded to C12, C14, and C15 were omitted from the refinement. The remaining 44 independent hydrogen atoms were treated as described for **1**. The final agreement factors[26] were $R = 0.049$ and $R_w = 0.062$ for the 2244 reflections having $I \geq 3\sigma_I$.

Results

X-ray Studies. The atom-labeling scheme for **1** is given in the ORTEP plot of Figure 1 while selected bond lengths and angles are

---

(23) Sau, A. C.; Day, R. O.; Holmes, R. R. *Inorg. Chem.* **1981**, *20*, 3076.

(24) The function minimized was $\sum w(|F_o| - |F_c|)^2$, where $w^{1/2} = 2F_oLp/\sigma_I$.

(25) *International Tables for X-ray Crystallography*; Kynoch: Birmingham, England, 1969; Vol. I, p 167.

(26) $R = \sum||F_o| - |F_c||/\sum|F_o|$ and $R_w = [\sum w(|F_o| - |F_c|)^2/\sum w|F_o|^2]^{1/2}$.

(27) Reference 25, p 75.

(28) Reference 25, p 99.

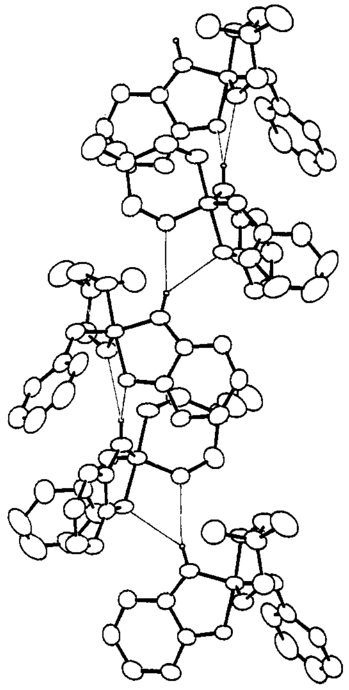

Figure 2. ORTEP plot of **1** showing the hydrogen-bonded helical chain formed by 4_1 screw related molecules. Hydrogen-bonding interactions are shown as narrow lines. Methyl groups on the xylyloxy substituents are omitted for clarity.

presented in Table I. The analogous information for **2** and **3** is given in Figure 3 and Table II and in Figure 5 and Table III. For all three compounds atomic coordinates, anisotropic thermal parameters, hydrogen atom parameters, and a complete tabulation of bond lengths and angles for non-hydrogen atoms are provided as supplementary material.

NMR Studies. Analysis of variable-temperature ^{1}H and ^{13}C NMR spectra yielded activation energies, $\Delta G^{\ddagger}$,[29] that are reported in Table IV along with the coalescence temperatures (T_c) and line separations ($\Delta\nu$) used in the calculations.

Discussion

Synthesis and Basic Structures. All three new tetraoxyphosphoranes, **1–3**, were formed by the oxidative addition of an *o*-aminophenol to the monocyclic phosphite **4** at −55 to −65 °C in diethyl ether solution. The reaction, conducted at low temperatures for 10 min, was completed at room temperature, eq 1.

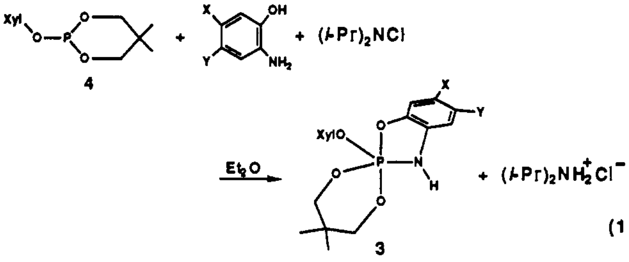

(1)

(1) X=Y=H; (2) X=H, Y=Me; (3) X=Me, Y=H

Intermolecular N–H---O hydrogen bonding exists in all three solid-state structures. This gives rise to helical chain for **1** and the presence of dimeric units for **2** and **3**. The geometry about the five phosphorus centers in all three compounds can be referred to a trigonal bipyramid (TBP) with the ring systems spanning axial-equatorial sites and the nitrogen atom of the iminophenolate ligand as well as the oxygen atom of the xylyloxy group in the equatorial plane.

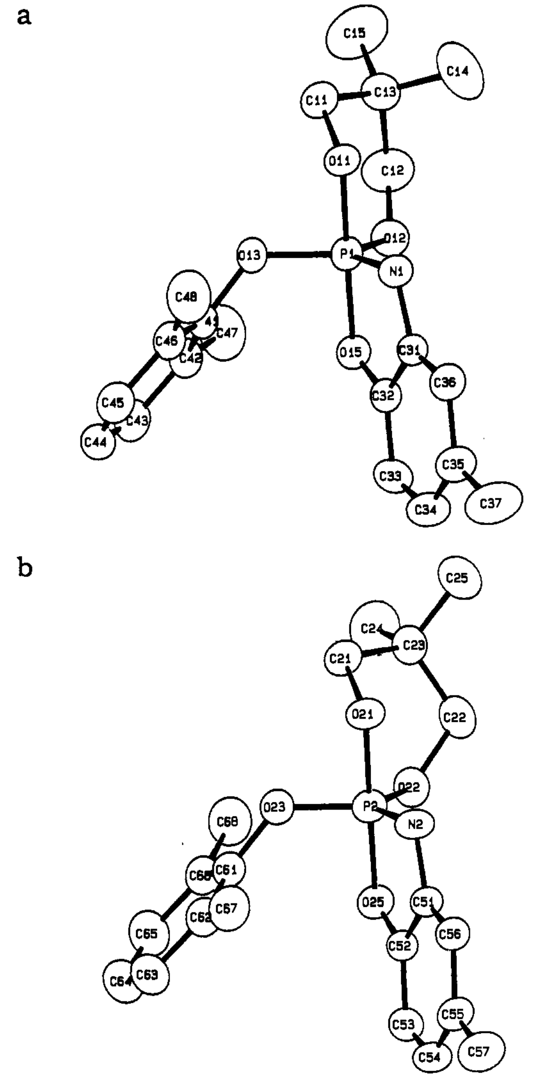

Figure 3. ORTEP plot of $(C_5H_{10}O_2)(Xyl\text{-}O)P(1\text{-}O\text{-}2\text{-}NH\text{-}4\text{-}MeC_6H_3)$ (**2**) with thermal ellipsoids at the 30% probability level: (a) the independent molecule which has the phosphorinane ring in the twist-chair conformation; (b) the independent molecule which has the phosphorinane ring in the twist-boat conformation. Hydrogen atoms are omitted for clarity.

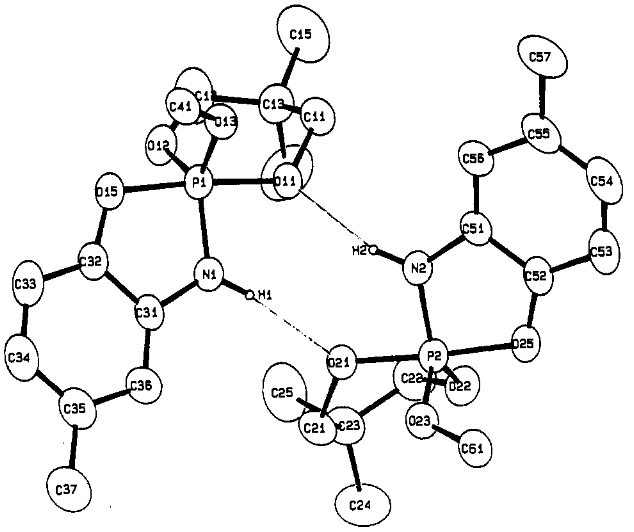

Figure 4. ORTEP plot of **2** showing the hydrogen-bonded dimer. Pendant carbon atoms of the xylyl groups and all but the imine hydrogen atoms are omitted for clarity.

Distortions away from the ideal TBP geometry do not follow the Berry pseudorotation coordinate but are, rather, slightly "anti"

---

(29) Calculated from the equation $\Delta G^{\ddagger}_c = (4.57 \times 10^{-3})T_c(10.32 + \log(T_c\sqrt{2}/\pi\Delta\nu))$ following: Kessler, H. *Angew. Chem.* **1970**, *82*, 237. See also: Buono, G.; Llinas, J. R. *J. Am. Chem. Soc.* **1981**, *103*, 4532.

Table II. Selected Distances (Å) and Angles (deg) for **2**[a]

atom 1	atom 2	distance	atom 1	atom 2	distance	atom 1	atom 2	distance	atom 1	atom 2	distance
P1	O11	1.670 (2)	P2	O25	1.711 (2)	N1	C31	1.403 (4)	C23	C24	1.542 (9)
P1	O12	1.586 (2)	P2	N2	1.642 (4)	C11	C13	1.516 (4)	C23	C25	1.522 (6)
P1	O13	1.614 (3)	O11	C11	1.433 (5)	C12	C13	1.497 (5)	C31	C32	1.381 (6)
P1	O15	1.713 (2)	O12	C12	1.405 (6)	C13	C14	1.537 (9)	H1	O21	2.09 (4)
P1	N1	1.660 (4)	O15	C32	1.355 (6)	C13	C15	1.501 (8)	H1	N1	0.84 (4)
P2	O21	1.677 (2)	O21	C21	1.444 (5)	C21	C23	1.535 (5)	H2	O11	2.05 (4)
P2	O22	1.600 (3)	O22	C22	1.463 (3)	C22	C23	1.514 (6)	H2	N2	0.85 (3)
P2	O23	1.607 (3)							C51	C52	1.367 (7)

atom 1	atom 2	atom 3	angle	atom 1	atom 2	atom 3	angle	atom 1	atom 2	atom 3	angle
O11	P1	O12	96.6 (1)	O25	P2	N2	88.8 (1)	C14	C13	C15	110.5 (5)
O11	P1	O13	89.7 (1)	P1	O11	C11	120.8 (2)	O21	C21	C23	110.0 (3)
O11	P1	O15	174.5 (2)	P1	O12	C12	128.7 (1)	O22	C22	C23	112.8 (3)
O11	P1	N1	86.9 (1)	P1	O15	C32	114.3 (2)	C21	C23	C22	107.5 (3)
O12	P1	O13	112.7 (2)	P2	O21	C21	117.2 (3)	C21	C23	C24	108.4 (4)
O12	P1	O15	87.7 (1)	P1	N1	H1	120. (3)	C21	C23	C25	111.1 (3)
O12	P1	N1	122.7 (1)	C31	N1	H1	124. (3)	C22	C23	C24	111.1 (4)
O13	P1	O15	91.8 (1)	P1	O11	H2	126. (1)	C22	C23	C25	108.6 (4)
O13	P1	N1	124.6 (1)	C11	O11	H2	111. (1)	C24	C23	C25	110.1 (4)
O15	P1	N1	87.9 (1)	P2	O22	C22	119.7 (2)	N1	C31	C32	108.0 (4)
O21	P2	O22	94.4 (1)	P1	N1	C31	116.8 (3)	O15	O32	C31	112.7 (3)
O21	P2	O23	89.4 (1)	O11	C11	C13	109.7 (3)	N2	C51	C52	107.7 (4)
O21	P2	O25	176.0 (2)	O12	C12	C13	118.8 (4)	O25	C52	C51	112.8 (3)
O21	P2	N2	87.3 (1)	C11	C13	C12	107.2 (3)	O21	H1	N1	170. (5)
O22	P2	O23	112.4 (2)	C11	C13	C14	109.6 (4)	O11	H2	N2	160. (4)
O22	P2	O25	88.6 (1)	C11	C13	C15	111.5 (4)	P2	N2	H2	120. (3)
O22	P2	N2	124.2 (2)	C12	C13	C14	108.7 (4)	C51	N2	H2	123. (3)
O23	P2	O25	92.0 (1)	C12	C13	C15	109.3 (4)	P2	O21	H1	131. (1)
O23	P2	N2	123.3 (1)					C21	O21	H1	112. (1)

[a] Estimated standard deviations in parentheses. The atom-labeling scheme is shown in Figure 3.

Table III. Selected Distances (Å) and Angles (deg) for **3**[a]

atom 1	atom 2	distance	atom 1	atom 2	distance	atom 1	atom 2	distance	atom 1	atom 2	distance
P1	O11	1.669 (4)	P2	O25	1.720 (5)	N1	C31	1.387 (8)	C23	C24	1.53 (1)
P1	O12	1.601 (4)	P2	N2	1.646 (4)	C11	C13	1.53 (1)	C23	C25	1.537 (9)
P1	O13	1.606 (4)	O11	C11	1.437 (8)	C12A	C13	1.53 (2)	C31	C32	1.390 (7)
P1	O15	1.712 (4)	O12	C12A	1.46 (1)	C12B	C13	1.46 (2)	C51	C52	1.388 (8)
P1	N1	1.658 (4)	O12	C12B	1.52 (2)	C13	C14	1.46 (1)	H1	N1	0.87 (5)
P2	O21	1.671 (4)	O15	C32	1.359 (7)	C13	C15	1.45 (1)	H1	O21	2.05 (5)
P2	O22	1.592 (4)	O21	C21	1.425 (7)	C21	C23	1.54 (1)	H2	O11	2.13 (5)
P2	O23	1.607 (4)	O22	C22	1.439 (9)	C22	C23	1.53 (1)	H2	N2	0.76 (6)

atom 1	atom 2	atom 3	angle	atom 1	atom 2	atom 3	angle	atom 1	atom 2	atom 3	angle
O11	P1	O12	96.1 (2)	P1	O11	C11	120.2 (3)	C11	C13	C15	110.8 (6)
O11	P1	O13	88.9 (2)	P1	O12	C12A	121.4 (5)	N2	C51	C52	109.6 (5)
O11	P1	O15	174.7 (2)	P1	O12	C12B	130.8 (7)	C12A	C13	C14	121.4 (8)
O11	P1	N1	86.8 (2)	O25	C52	C51	111.3 (5)	C12A	C13	C15	91.3 (9)
O12	P1	O13	113.0 (2)	C24	C23	C25	111.6 (7)	C12B	C13	C14	89.6 (8)
O12	P1	O15	88.5 (2)	N1	C31	C32	109.0 (4)	C12B	C13	C15	127 (1)
O12	P1	N1	122.0 (3)	O15	C32	C31	112.0 (5)	C14	C13	C15	111.3 (8)
O13	P1	O15	91.8 (2)	P1	N1	H1	123. (4)	O21	C21	C23	110.5 (5)
O13	P1	N1	124.9 (2)	C31	N1	H1	121. (4)	O22	C22	C23	113.2 (6)
O15	P1	N1	88.5 (2)	P1	O11	H2	124. (2)	C21	C23	C22	106.5 (6)
O21	P2	O22	95.2 (2)	C11	O11	H2	113. (2)	C21	C23	C24	109.6 (6)
O21	P2	O23	89.6 (2)	P1	O15	C32	114.0 (3)	C21	C23	C25	109.4 (6)
O21	P2	O25	176.1 (2)	P2	O21	C21	117.0 (3)	C22	C23	C24	109.4 (7)
O21	P2	N2	88.1 (2)	P2	O22	C22	119.0 (4)	C22	C23	C25	110.3 (6)
O22	P2	O23	112.9 (2)	P1	N1	C31	116.4 (3)	O11	H2	N2	169. (6)
O22	P2	O25	88.3 (2)	O11	C11	C13	110.7 (6)	O21	H1	N1	173. (5)
O22	P2	N2	122.7 (3)	O12	C12A	C13	113.2 (9)	P2	N2	C51	116.7 (4)
O23	P2	O25	90.7 (2)	O12	C12B	C13	113.7 (9)	P2	N2	H2	118. (4)
O23	P2	N2	124.3 (2)	C11	C13	C12A	110.6 (7)	C51	N2	H2	124. (5)
O25	P2	N2	88.4 (2)	C11	C13	C12B	105.5 (8)	P2	O21	H1	129. (2)
				C11	C13	C14	110.0 (7)	C21	O21	H1	113. (2)

[a] Estimated standard deviations in parentheses. The atom-labeling scheme is shown in Figure 5.

Berry in nature. The latter feature is occasionally found when, as here, the distortions from ideal symmetry are not too large.[30] In all cases, the axial oxygen atoms are tipped toward the nitrogen atom with O_{axial}–P–O_{axial} angles ranging from 174.5 (2)° to 176.1 (2)°. This distortion is due in part to the constraints imposed by the five-membered rings wherein the O–P–N angles range from 87.6 (2)° to 88.8 (1)°. Accompanying this distortion, the $O_{equatorial}$–P–$O_{equatorial}$ angles are "closed down" from 120° with values that range from 112.4 (2)° to 113.5 (2)°.

The five-membered rings in all three compounds are essentially planar. In compound **1** the atoms P, N, O5, C11, and C12 are coplanar to within ±0.012 Å. For compound **2** the corresponding values are ±0.033 Å for the molecule containing P1 and ±0.051

---

[30] (a) Holmes, R. R. *Prog. Inorg. Chem.* **1984**, *32*, 119. Refer to pp 151 and 209. (b) Holmes, R. R. *Pentacoordinated Phosphorus, Structure and Spectroscopy*; ACS Monograph 175; American Chemical Society: Washington, DC, 1980; Chapter 2.

Table IV. Activation Parameters of Ligand Exchange Determined from Variable-Temperature NMR Spectra

compd	temp range, °C	T_c, °C	$\Delta\nu$, Hz	$\Delta G^{\ddagger}{}_c$,^{a} kcal/mol
1	-85 to +15	-50	158.1	$10.3^{b,c}$
1	-75 to +25	-18	315.3	$11.5^{d,e}$
1	-75 to +25	-53	120	$10.4^{d,f}$
2	-95 to +20	-50	105	$10.5^{b,c}$
3	-88 to +17	-50	138	$10.4^{b,c}$
3	-75 to +45	-20	316	$11.4^{d,e}$

^{a}Values are estimated to be accurate to within ±1.5 kcal/mol. See ref 29. $^b\Delta G^{\ddagger}$ calculated from ^{1}H NMR spectra. $^c\Delta G^{\ddagger}$ calculated from coalescence of $C_6H_3(CH_3)_2$ signals. $^d\Delta G^{\ddagger}$ calculated from ^{13}C NMR spectra. $^e\Delta G^{\ddagger}$ calculated from coalescence of OCH_2 signals. $^f\Delta G^{\ddagger}$ calculated from coalescence of $C_6H_3(CH_3)_2$ signals.

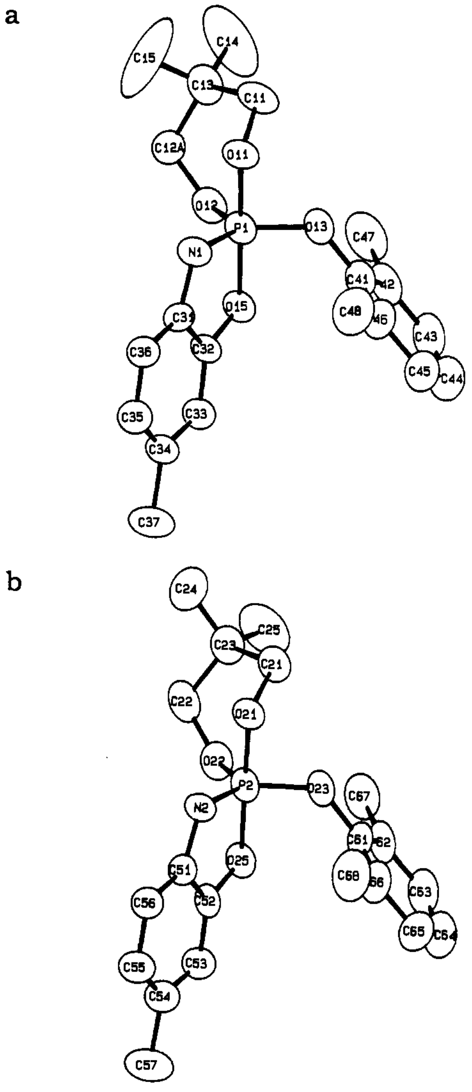

Figure 5. ORTEP plot of $(C_5H_{10}O_2)(Xyl\text{-}O)P(1\text{-}O\text{-}2\text{-}NH\text{-}5\text{-}MeC_6H_3)$ (3) with thermal ellipsoids at the 30% probability level: (a) the independent molecule with the disordered phosphorinane ring in its twist-boat conformation [C12B (forming a twist-chair conformation) is omitted for clarity]; (b) the independent molecule which has the phosphorinane ring in the twist-boat conformation. Hydrogen atoms are omitted for clarity.

Å for the molecule containing P2. For compound 3 these values are ±0.010 and ±0.015 Å.

Intermolecular Hydrogen Bonding. Hydrogen bonding involving the imino function gives rise to interesting structural variations. In compound 1, the imino hydrogen atom enters into a bifurcated hydrogen-bonding interaction with both the axial oxygen atom of the iminophenolate (O5) and the equatorial oxygen atom of the phosphorinane ring (O2) of a 4_1 screw related molecule. The propagation of this interaction by the 4_1 screw axis results in a hydrogen-bonded helical chain along *c* (Figure 2).

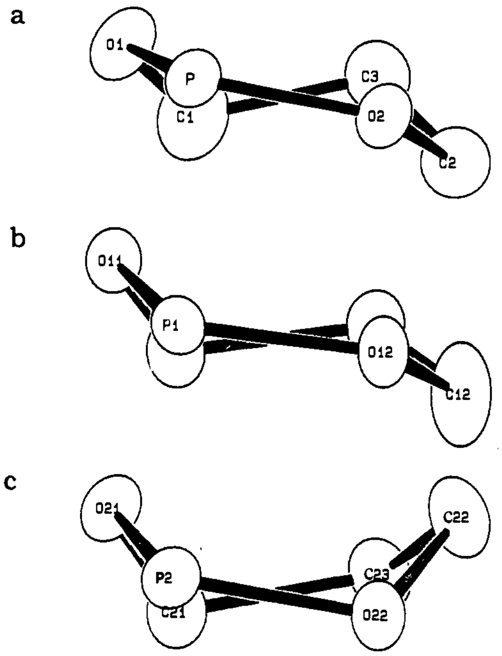

Figure 6. ORTEP plots showing the conformations of the phosphorinane rings in compounds 1 and 2: (a) the twist-chair conformation in 1; (b) the independent molecule in 2 which has the twist-chair conformation; (c) the independent molecule in 2 which has the twist-boat conformation.

In both compounds 2 and 3, there are two independent molecules in the asymmetric unit. These independent molecules are joined by two hydrogen bonds between the imino hydrogen atom from one and the axial oxygen atom of the phosphorinane ring from the other. Figure 4 shows this representative structure for 2. The idealized symmetry of the hydrogen-bonded dimers which are thus formed would be C_2, where the geometry at the phosphorus atom in both halves of the dimer has the same handedness.

The presence of the methyl groups in the cresol derivatives, 2 and 3, possibly could have led to a steric interaction if the helical form had prevailed, as in 1, and as a consequence yielded the observed dimer formulations. It is noted that in the helical turn of 1 (Figure 2) the aminophenol residues are located adjacent to each other in neighboring units in the chain, whereas in the dimers of both 2 and 3 the methyl-substituted aminophenol residues are adjacent to the six-membered rings (Figure 4 shows this for 2).

There is no compelling reason to believe that hydrogen-bonding interactions in solution must be different for the three compounds. The formation of hydrogen-bonded dimers in 1 is clearly possible. Insertion of dummy methyl group carbon atoms as substituents on atoms C14 and C15 in 1 shows no close intermolecular contacts *within the helix* for the carbon bonded to C14 (assuming a van der Waals' radius of 2.0 Å for the Me group). For the carbon bonded to C15 there are two such contacts (3.3 Å to both C33 and C34 of the xylyloxy group of an adjacent molecule). These contacts are not really prohibitive assuming some relaxation of the xylyloxy group orientation in solution and a van der Waals' sum of 3.7 Å. In solution where structural constraints are more relaxed, the possibility of equilibra among non-hydrogen-bonded and hydrogen-bonded forms also exists. The small NH doublet ($^2J_{(P-H)}$ coupling) at 5.3 ppm in the ^{1}H NMR spectrum of 1 at 15 °C (Figure 9) moves downfield on lowering the temperature. It appears as a broad peak at ~7.6 ppm at -85 °C. This suggests rapid exchange with a concentration toward hydrogen-bonded forms at low temperature.

Hydrogen-Bonded Phosphorinane Ring Conformations. The six-membered phosphorinane ring in 1 can be viewed as having a twist-chair conformation (Figure 6a).[31] Alternatively, the

---

(31) We use the term twist-chair rather than half-chair since O1-P-O2-C2 of Figure 6a do not lie in a plane. The nonplanarity of O11-P1-O12-C12 for the chair conformation of Figure 6b is even more evident. Also twist-chair vs twist-boat conformations are easier to visualize in the present context.

conformation of the ring can be described as a chair with considerable flattening at the phosphorus atom. The atoms O1, O2, C1, and C2 are coplanar to within ±0.059 Å, where the phosphorus atom and atom C3 are displaced in opopposite directions from this plane by distances of 0.340 and 0.744 Å, respectively.

In compound **2**, two different conformations for the phosphorinane ring are found. For the half of the dimer containing P1, the phosphorinane ring has a twist-chair conformation (Figure 6b), while for that containing P2 the conformation is that of a twist-boat (Figure 6c) with the axial oxygen atom in a prow position. Since the hydrogen bond is to the axial oxygen atom in each case, i.e., the dimer has idealized C_2 symmetry, it is unlikely that there is a large difference in energy between the two conformations. The conversion of one conformation to the other is easily visualized. Starting with the twist-boat accompanying P2, the prow carbon atom C22 is rotated away from the prow oxygen atom O21 about an axis passing through O22 and C23 until it reaches the position occupied by C12 in the twist-chair conformation. The effect of this conversion on the positions of the remaining ring atoms would be slight.

In **3**, as in **2**, the two phosphorinane rings are different (Figure 7). The conformation of the phosphorinane ring containing P2 is a twist-boat which is very similar to that found in **2**. The phosphorinane ring containing P1 is disordered, with two positions for atom C12 but only one resolvable position for the remaining ring atoms. When position C12A is occupied, the conformation of the ring is a twist-boat, but with position C12B occupied the conformation is a twist-chair. While the disorder appears static on the time scale of the X-ray experiment, dynamic interchanges between these positions correspond to the conversion of the boat conformation to the chair conformation discussed previously. The observed disorder in this ring reinforces the notion that the two conformations are close in energy.

Hydrogen-Bonded vs Non-Hydrogen-Bonded Phosphorinane Rings. The effects of hydrogen bonding on the conformation of the phosphorinane ring can be assessed by comparison to the related compounds, **5**, **6**, and **7**, in which hydrogen bonding is not present.[4] In these compounds, the phosphorinane ring also spans axial-equatorial sites of a trigonal bipyramid but has exclusively a near perfect boat conformation with the axial oxygen atom in a prow position.[4]

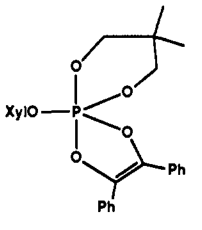

5

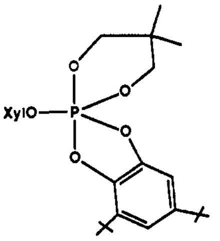

6

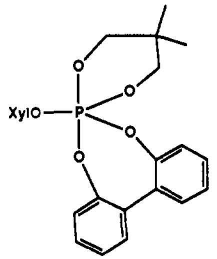

7

Despite the fact that the twist-boat conformation observed in **2** and **3** also has the axial oxygen atom in a prow position, the orientation of the boat in these compounds is different from that found in **5** through **7**. In the case of **2** and **3** the fold along the line between the prow atoms (Figure 8a, X = NH) is such that the 4-atom base of the boat is tipped toward the xylyloxy group and away from the NH function. This arrangement is most likely necessary to provide a lower energy path sterically for the hydrogen-bonding interaction. In the case of compounds **5** through **7**, the fold along the line between the prow atoms (Figure 8c, X = O) is such that the 4-atom base of the boat is tipped away from the xylyloxy group and toward position X, which could prevent an NH group in position X from entering into a hydrogen-bonding interaction by steric intervention.

The difference in the two types of orientation for the boat is apparent in the $X-P-O_A-C_A$ torsion angles defined in Figure 8 and given in Table V. For the boats in compounds **5** through **7**, this angle has values less than 69°, while for the twist boats in compounds **2** and **3**, this value exceeds 160°. The value of this angle for the twist chairs found in compounds **1** through **3** (Figure 8b) is similar to the value for the twist boats (in excess of 151°). This supports the notion that the primary difference in the chair and boat conformations is due to the placement of atom C_E which

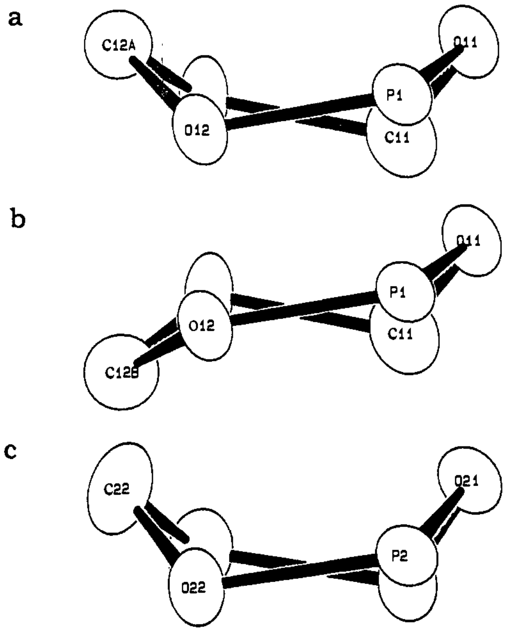

Figure 7. ORTEP plots showing the conformations of the phosphorinane rings in **3**: (a) the disordered ring in its twist-boat conformation; (b) the disordered ring in its twist-chair conformation; (c) the independent molecule which has only the twist-boat conformation.

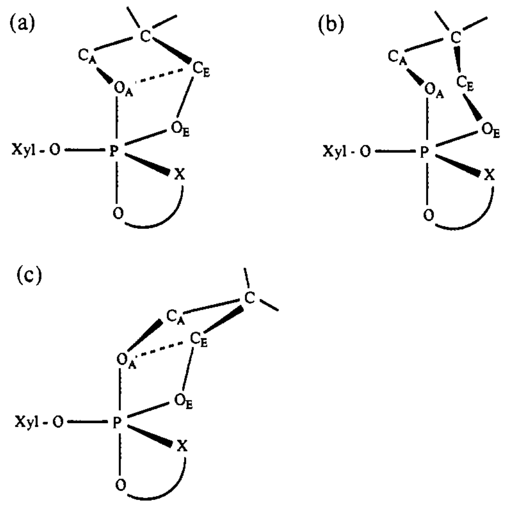

Figure 8. (a) Twist-boat as found in **2** and **3** (X = NH). The fold is along a line between "prow" atoms OA and CE such that CA is away from X. Torsion angle X-P-OA-CA > 90°. (b) Twist-chair as found in **1**-**3**. This conformation can be converted to a twist-boat by moving only atom CE into a prow position. The torsion angle $X-P-O_A-C_A$ is essentially unchanged (>90°). (c) Boat as found in **5**-**7** (X = O). The fold along the line between "prow" atoms OA and CE is such that CA is toward X. Torsion angle $X-P-O_A-C_A < 90°$.

Table V. Phosphorinane Torsion Angles for Hydrogen- and Non-Hydrogen-Bonded Phosphoranes

compd	torsion angle $X-P-O_A-C_A$,[c] deg	phosphorinane conformation
1[a]	151.1	twist-chair
2[a]	167.4	twist-boat
2[a]	166.5	twist-chair
3[a]	168.5	twist-boat
3[a]	160.8	twist-boat/chair[d]
5[b]	68.1	boat
6[b]	63.5	boat
7[b]	68.4	boat

[a] This work. [b] Reference 4. [c] Defined in Figure 9. [d] Disordered ring.

Table VI. Dihedral Angles between P–O_{eq}–C Planes and Equatorial Planes for Spirocyclic Phosphoranes (deg)

	ring size, no. of atoms			xylyloxy group	phosphorinane conformation
	5	6	7		
1[a]	88.2	72.5		89.8	twist-chair
2[a]	83.8	64.1		89.0	twist-boat
2[a]	87.8	63.9		74.5	twist-chair
3[a]	90.0	67.1		86.4	twist-boat
3[a]	89.7	63.4/67.9		85.3	twist-boat/chair[c]
5[b]	87.9	75.9		87.8	boat
6[b]	79.0	86.4		88.2	boat
7[b]		77.8	66.6	72.5	boat

[a] This work. [b] Reference 4. [c] Disordered ring.

Table VII. Comparison of Ring and Acyclic P–O Bond Lengths (Å) for Phosphoranes **1–3**

compd	six-membered ring P–O_{ax}	six-membered ring P–O_{eq}	five-membered ring P–O_{ax}	acyclic P–O_{eq}
	hydrogen bonded			
1[a]		1.586	1.740	
2[a]	1.670			
2[b]	1.677			
3[a,b]	1.669			
3[b]	1.671			
	non-hydrogen bonded			
1[a]	1.648			1.615
2[a]		1.586	1.713	1.614
2[b]		1.600	1.711	1.607
3[a,b]		1.601	1.712	1.606
3[b]		1.592	1.720	1.607

[a] Twist-chair. [b] Twist-boat.

apparently has no effect on the stereochemistry of the hydrogen bonding.

One may conclude that the lowest energy conformation for the phosphorinane ring is the boat (**8c**) found thus far in all compounds where no hydrogen bonding is present. The difference in energy between this conformation and the less stable twist boat (or chair) is low enough that hydrogen-bonding interactions are sufficient to cause the conversion to the latter.

An interesting consequence of hydrogen bonding found in **1–3** is the presence of lower dihedral angles between the P–O_{eq}–C planes and the equatorial planes for phosphorinane rings compared to that formed for the phosphorinane rings in the related spirocyclics, **5–7**[4] (Table VI). Trippett[16] concluded that a six-membered ring in a boat conformation located in axial-equatorial positions of a trigonal bipyramid would be the most stable since this is the only structure that allows the P–O_{eq}–C plane to be perpendicular to the equatorial plane. The latter 90° angle maximizes the preference[32] of the lone pairs on the equatorial ring heteroatom to be located in the equatorial plane. For the boat conformations of the phosphorinane rings of the oxyphosphoranes that lack hydrogen bonding, **5–7**, this condition is approached, as is evident from the range of dihedral angles, 76–86°, approaching 90°. These compare with the values for the dihedral angles found for the xylyloxy groups which are free of any ring constraint. The hydrogen-bonded spirocyclics, **1–3**, however, independent of whether a chair or boat form is situated axial-equatorially, show considerably lower phosphorinane dihedral angles: 64–68° for the dimeric molecules, **2–3**, and 72.5° for the helical structure, **1** (Table VI). This reduction relates to the form of the twist boat (Figure 8a) or chair (Figure 8b) stabilized in the hydrogen-bonded phosphoranes, **1–3**, in contrast to the boat conformation normally formed for phosphorinane rings in the absence of hydrogen-bonding interactions (Figure 8c). It is interesting to note that in tetracoordinate phosphorus compounds containing dithiaphosphorinane rings, there is a propensity of molecules indicated to have these rings in a twist-boat conformation.[33]

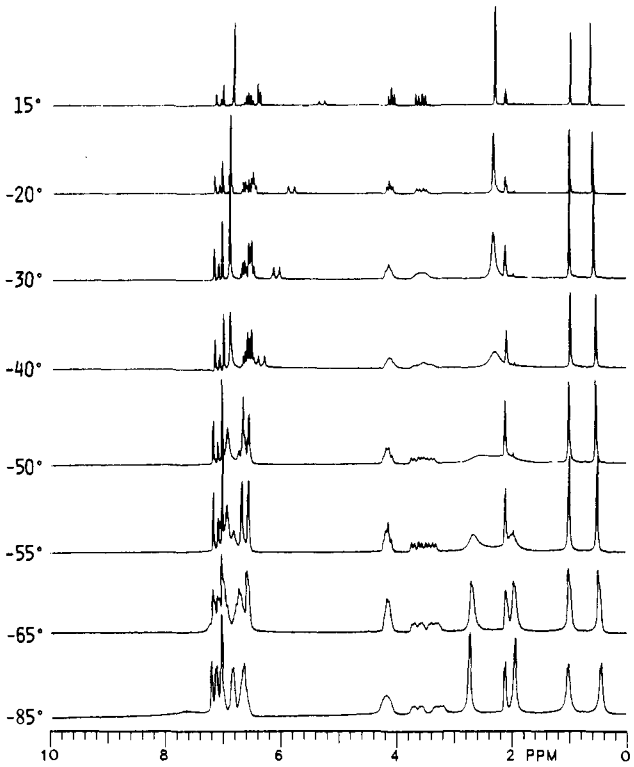

Figure 9. Variable-temperature ^{1}H NMR spectrum of **1**. The signal at 2.1 is due to the solvent, toluene-d_8.

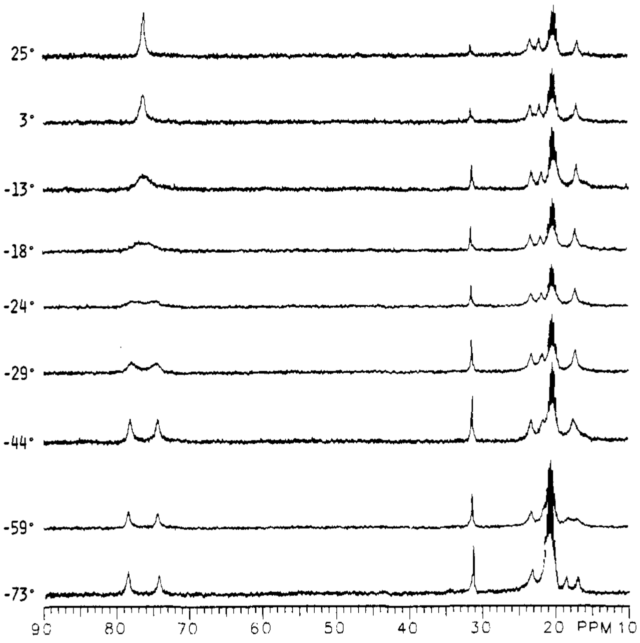

Figure 10. Variable-temperature ^{13}C NMR spectrum of **1** in toluene-d_8.

Comparison of P–O bond lengths for **1–3** in Table VII shows that the hydrogen-bonded P–O axial bonds in the five- and six-membered rings average 0.02–0.03 Å longer than corresponding bonds that are not hydrogen bonded. Similar to previous work,[1b,4,5] the P–O axial bonds average about 0.06 Å longer in the more strained unsaturated five-membered rings compared to the saturated six-membered rings situated in axial-equatorial sites. However, no significant differences are apparent between hydrogen-bonded P–O axial bond lengths for chair and boat conformations so that a conformational effect ascribed to this feature is excluded.

---

(32) Hoffmann, R.; Howell, J. M.; Muetterties, E. L. *J. Am. Chem. Soc.* **1972**, *94*, 3047.

(33) Maryanoff, B. E.; Hutchins, R. O.; Maryanoff, C. A. *Top. Stereochem.* **1979**, *11*, 187 and references cited therein.

Scheme I

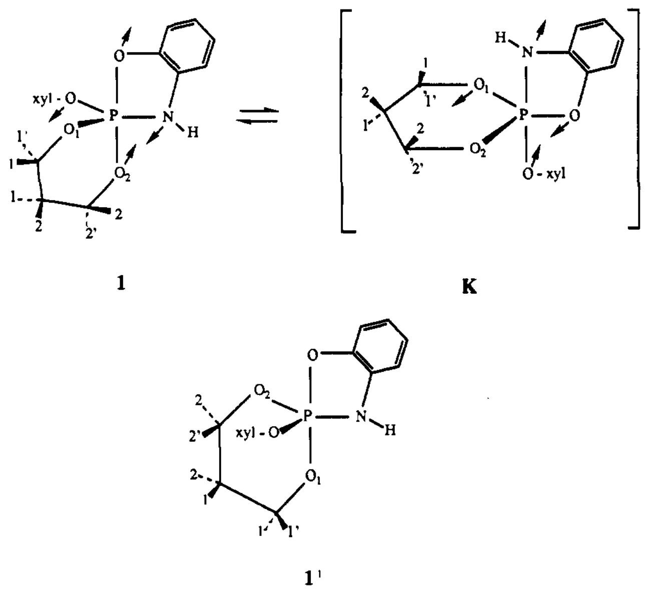

1 **K** **1'**

NMR and Intramolecular Ligand Exchange. Figures 9 and 10 display the variable-temperature ^1H and ^{13}C NMR spectra of **1**, respectively, in $C_6D_5(CD_3)$ solution. ^{31}P NMR chemical shifts for **1–3**, all near −58 ppm, establish that the compounds remain as phosphoranes in solution. Proceeding from right to left, the ^1H NMR spectrum at 15 °C (Figure 9) shows the phosphorinane ring methyl doublet, a small peak due to toluene-d_8, the xylyloxy methyl singlet, two multiplets attributable to the methylene groups of the six-membered ring, a small NH doublet, and a number of peaks in the aromatic region. Assignments at 25 °C in the ^{13}C NMR spectrum of **1** in Figure 10, proceeding from right to left, are carbon peaks due to the xylyloxy methyl (singlet), toluene-d_8 (multiplet), phosphorinane ring methyls (two singlets), phosphorinane bridge carbon (singlet), and the methylenes of the phosphorinane ring (singlet). Similar spectra were recorded for **2** and **3**. At lower temperatures, both the ^1H and ^{13}C spectra have more complex patterns exhibiting two O-Xyl signals instead of one and an increase in the number of ring methylene signals. However, in each spectrum, the number of phosphorinane methyl signals remains invariant at two. Further it is seen that the NH doublet ($^2J_{P-H}$ coupling) moves downfield as the temperature is lowered.

Analysis of the coalescence of various peaks yielded the activation energies in Table IV which do not vary significantly whether they were obtained from the ^{13}C or ^1H spectra and also appear to be independent of which peak is under consideration. The latter implies that C–O bond rotation, which equilibrates the O-Xyl methyl groups, accompanies the intramolecular ligand exchange process which equilibrates the phosphorinane methylene groups.[4,5] $^3J_{P-H}$ coupling of multiplets associated with the latter groups supports the process as intramolecular.

The variable-temperature ^1H and ^{13}C NMR spectra for **1** are interpretable in terms of a Berry pseudorotational process[15] which places the six-membered ring diequatorially in an exchange intermediate.[34] As seen in Scheme I, the first exchange ($1 \rightleftharpoons K$) via an intervening square pyramid, where O_1 acts as the pivotal ligand (i.e., O_1 becomes apical in the square-pyramidal form), is followed by exchange ($K \rightleftharpoons 1'$) via an intervening square pyramid, where O_2 serves as the pivotal ligand. Comparison of **1** and **1'** shows that the four inequivalent CH_2 protons and the protons of the xylyloxy CH_3 groups of **1** should coalesce to a pattern indicative of two CH_2 protons and one type of xylyloxy methyl proton, whereas the protons of the two six-membered-ring methyl groups remain inequivalent. Likewise, the carbons of the two CH_2 groups and the carbons of the two methyl substituents of the O-Xyl groups become equivalent in **1** and **1'**, whereas the carbon atoms of the two six-membered-ring methyl groups remain inequivalent in **1** and **1'**.[35] Essentially this behavior is observed in Figures 9 and 10, although the pattern for the four methylene protons, expected to be four ABX quartets (where X = P), is not completely resolved in Figure 9. The best resolution is seen at −55 °C where an eight-line multiplet, corresponding to two ABX patterns, and a lower field broad multiplet, most likely encompassing the other two ABX components, are present.[36]

The activation energies (ΔG^*) of 10.3–11.5 kcal/mol for exchange via a six-membered ring for the trigonal bipyramids of **1–3** (Table IV) are not significantly different as might be anticipated for these closely related phosphoranes and are higher than the 6.1 kcal/mol Trippett[16] observed for J (shown in the Introduction) but comparable to that reported[4] for L, i.e., 11.8 kcal/mol. The exchange intermediate corresponds to K in Scheme I, for L would have the less electronegative phenyl group in an axial position, thus tending to increase the barrier. For **1–3**, the more sterically demanding xylyloxy group[5] relative to the phenoxy substituent in J may serve to raise the exchange barrier.

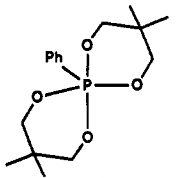

L

Conclusion

The use of hydrogen bonding, as introduced in this study, as a factor in altering the structure of oxyphosphoranes, which serve as models for the enzymatic and base-catalyzed hydrolysis of c-AMP, produced conformational changes in the six-membered rings which resulted in a chair form rather than the usually observed boat form while maintaining the rings in axial-equatorial positions of a trigonal bipyramid. It is inferred that the energy required to induce diequatorial phosphorinane ring formation in the systems under study here (≥11 kcal/mol) exceeds the available hydrogen-bonding energy. It is not inferred that an enzyme-active site does not have sufficient constraints, hydrogen bonding as well as others, to induce diequatorial formation in a c-AMP intermediate. Further studies are needed to fully appreciate the factors that might allow a diequatorial site preference for phosphorinane rings of oxyphosphoranes that exist as trigonal bipyramids.

Acknowledgment. The support of this research by the National Science Foundation (Grant CHE88-19152) and the Army Research Office is gratefully acknowledged.

Supplementary Material Available: Tables of thermal parameters, additional bond lengths and angles, hydrogen atom parameters (Tables S1–S3 for **1**, Tables S4–S6 for **2**, and Tables S7–S9 for **3**), and atomic coordinates (Tables S10–S12 for **1–3**, respectively) (33 pages). Ordering information is given on any current masthead page.

---

(34) Reference 30b, p 163.

(35) Exchange via an intermediate with the five-membered ring occupying diequatorial positions is ruled out as this exchange process would equilibrate the phosphorinane ring methyl signals in both the ^1H and ^{13}C spectra above the coalescence temperatures. Exchange via the five-membered-ring intermediate must be preceded or followed by a simple axial-equatorial ring pseudorotation to locate the ring nitrogen in an equatorial position.

(36) For **2**, the methylene region shows greater resolution. At −65 °C, fifteen of the sixteen expected lines are discernible.